10 Electron Nanodiffraction

10.1 Introduction

Here, electron nanodiffraction refers to a set of electron diffraction techniques that enable structural analysis at nanoscale. Specifically, the techniques we discuss here extend the study of electron diffraction to nanostructures, 'small' crystals, defects and material's microstructure. We show how such studies can be carried quantitatively at spatial resolutions ranging from sub-Å to nm and in 2D projections to 3D reconstruction.

Many of the instrumental requirements for electron nanodiffraction are similar to those for analytical electron microscopy. In fact, modern analytical TEMs provide special convergent beam electron diffraction (CBED) or nanobeam modes, or both, together with the modes for low and high magnification TEM, diffraction, and EDX. This development resulted partly from the fact that the requirements for EDX (large tilt, small probe, low contamination) exactly match those for nanodiffraction. Analytical TEMs designed for STEM also feature a brighter field emission gun (FEG), an improved vacuum system and instrument stability required for electron nanodiffraction. Most importantly, there is a clear scientific merit here since microanalysis complements electron diffraction in analytical TEM by providing both chemical and crystallographic information.

The predecessor of electron nanodiffraction is electron microdiffraction using CBED. The first CBED pattern was recorded by Möllenstadt as early as 1939 using a two magnetic lenses setup [1]. MacGillavry first attempted structure factor measurement by using the two-beam theory of Blackman for dynamic electron diffraction [2]. The multi-beam theory of electron dynamic diffraction has its origin in the Bloch wave method originally formulated by Hans Bethe in his Ph.D. thesis. Electron nanodiffraction started with the development of field emission guns (FEG) in the 70's, which led to the development of dedicated STEM. Electron nanodiffraction took advantage of the small and highly coherent electron beam in these instruments (see Cowley's reviews [3, 4]). However, in these early STEMs, diffraction patterns were often recorded using the TV cameras and on video tapes; the quality of recorded diffraction patterns was poor and the handling of video data was difficult. The development of array detectors, such as CCD cameras or imaging plates, enabled parallel recording of diffraction patterns and quantification of diffraction intensities over a large dynamic range that became widely available only in 1990s[5, 6]. At above the same time, field emission instruments that combines STEM with TEM were developed. Electron energy filters, such as the in-column Ω-energy-filter, also became available that allowed the inelastic background from plasmon, or higher electron energy losses, to be removed from recorded diffraction patterns with an energy resolution of a few eV [7]. These developments in electron diffraction

hardware were accompanied by the development of efficient and accurate algorithms to simulate electron diffraction patterns[8] and modeling structures on a first-principle basis. By late 1990s, many technical difficulties encountered in performing electron nanodiffraction using dedicated STEM[3] have been solved. Other more recent developments are time-resolved electron diffraction at the time resolution approaching femtoseconds [9],[10],[11], coherent nanoarea electron diffraction for the study of individual nanostructures [12], electron diffraction using fast pixelated detector or segmented detectors[13, 14]. Further developments of these techniques will significantly improve our ability to interrogate structures at high spatial and time resolution that hitherto has not been available before.

This chapter provides a comprehensive coverage of electron nanodiffraction. The intention is to treat the topic in a reference format that readers will find useful as a guide for materials characterization using electron nanodiffraction. The chapter is organized in 6 sections. In section 2, various electron nanodiffraction techniques are described. This is followed by a discussion on electron probe formation in section 3 and energy filtering in section 4. The section 5 is on diffraction analysis. This part covers three major aspects: 1) diffraction pattern indexing and mapping, 2) CBED and 3) coherent electron nanodiffraction. Examples included in section 5 illustrate the applications of orientation mapping, strain analysis, 3D nanostructure determination, crystal local symmetry determination, structure factor measurements and diffractive imaging. Section 6 provides a brief conclusion.

Some background on transmission electron microscopy are needed, introductory materials and theoretical background that are not covered here can be found in several books [8, 15-18].

10.2   Electron diffraction techniques

10.2.1   Selected area electron diffraction (SAED)

Selected area electron diffraction is performed by illuminating the sample with a large defocused electron beam. The diffraction pattern is recorded from a selected sample area by placing an aperture at the image plane of the objective lens as shown in Figure 10.1. This plane is conjugate to the sample. Only electron beams passing through this aperture contribute to the diffraction pattern seen by the next intermediate lens. The electron beams come from the sample area defined by the virtual image of the selected area aperture at the specimen level. For an ideal lens, with the aperture centered on the optic axis, a small area at the center of the observed area is selected. This area is much smaller than the size of the aperture image because of the objective lens magnification. A TEM equipped with an imaging (not probe) aberration corrector comes close to providing an ideal objective lens. Without the corrector, rays belonging to diffracted beams are at an angle to the optic axis and they are displaced away from the center because of the spherical aberration of the objective lens (C_s). The displacement is proportional to $C_s\alpha^3$, where α is twice the Bragg

angle (Figure 10.1). The smallest area that can be selected in SAED is thus limited by the objective lens aberrations. This limitation is largely removed when using an electron microscope equipped with a TEM aberration corrector placed after the objective lens.
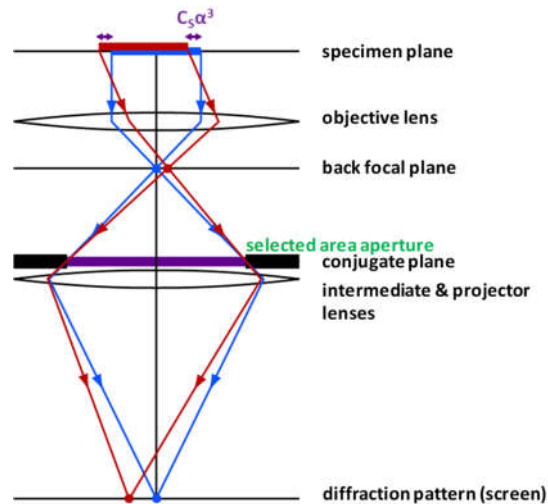

Figure 10.1 Schematic illustration of selected area electron diffraction in conventional TEM. (Provided by Jun Yamasaki of Nagoya University, Japan)
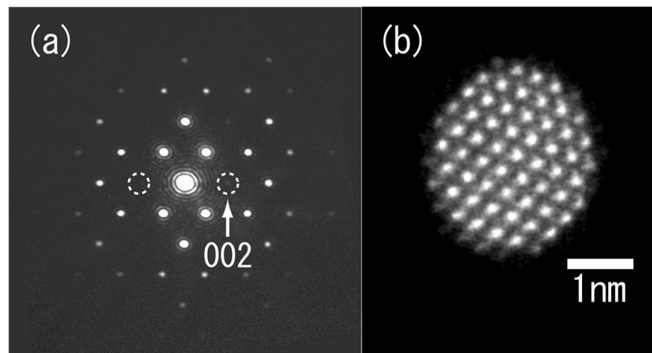

Figure 10.2 Selected area diffraction in an aberration corrected TEM. a) Diffraction pattern recorded from a silicon crystal along [110]. b) TEM image of the selected area on the silicon crystal. The aperture hole is 240 nm in diameter, which was fabricated in a copper thin plate using focused ion beams (FIB). (From [19], reproduced with permission)

SAED is the most popular diffraction technique in TEM. The technique can be applied to study both crystalline and noncrystalline materials. The large area illumination is useful for recording diffraction patterns from polycrystalline samples or for averaging over a large volume (for example, a large number of nanoparticles). SAED can also be used for low-dose electron diffraction, which is required for studying radiation sensitive materials, such as organic molecules. For small area analysis, the nanoarea electron diffraction technique described next is more appropriate. Alternatively, an aberration corrected TEM coupled with a small aperture can be used for electron nanodiffraction. For example, Morishita et al. demonstrated that coherent diffraction can be achieved from areas as small as ~10 nm using this technique ([19], also see Figure 10.2).

10.2.2 Nanoarea Electron Diffraction (NAED) and Nanobeam diffraction (NBD)

NAED uses a nanometer-sized parallel beam, with the condenser/objective setup shown in Figure 10.3 [12], together with the use of a small condenser aperture. An auxiliary condenser lens, called condenser minilens or CM, placed immediately above the condenser-objective lens is also employed [20]. The CM lens takes the crossover formed by the last condenser lens (CL) and images it onto the front focal plane of the objective pre-field lens, which then forms a parallel beam on the specimen. Adjustment to the parallel beam can be made by changing the CL and CM lens excitations; the CL lens moves the beam crossover closer or further away from the CM lens and thus changing the beam divergence angle seen by the CM lens. For a condenser aperture of 10 microns in diameter, the probe diameter is ~50 nm with an overall magnification factor of 1/200 in the JEOL 2010 or 2100 electron microscopes (JEOL, USA). The beam size is much smaller than what can be achieved using a selected area aperture. Diffraction patterns recorded in this mode are similar to the SAED patterns. For crystals, the diffraction pattern consists of sharp diffraction spots. The major difference is that the diffraction volume is defined directly by the electron probe in NAED since most electrons illuminating the sample are recorded in the diffraction pattern. NAED in a FEG microscope also provides higher beam intensity than SAED (the probe current intensity using a 10 micron condenser II aperture in a JEOL 2010F is ~10^5 e/s-nm^2) [12]. The small beam size allows the selection of an individual nanostructure and reduction of the background in the electron diffraction pattern from the surrounding materials. Figure 10.4 shows an example. The diffraction pattern was recorded from a single wall carbon nanotube encapsulated with C60 molecules using a 25 nm diameter electron probe (Figure 10.4a). The diffraction lines marked by the arrows are from C60 molecules. Together, ~25 C60 molecules were selected and contributed to diffraction.
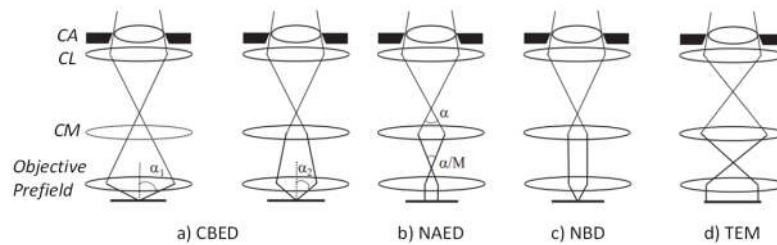
Figure 10.3 Comparison between CBED, NAED, NBD and TEM illumination for SAED. The sample is located at the lower end of the diagrams.
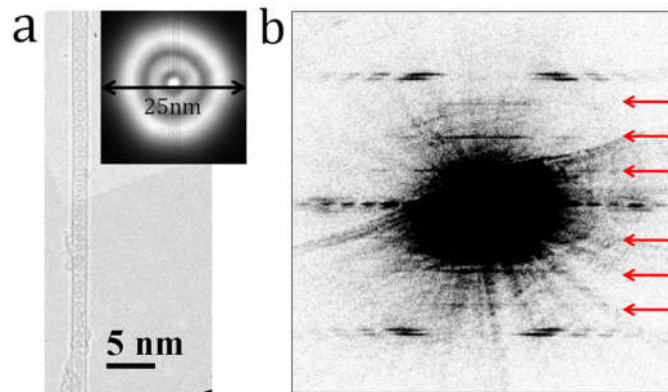

Figure 10.4 Nanoarea electron diffraction of a small diameter peapod (C60 molecules encapsulated inside a single wall carbon nanotube). (a) High Resolution TEM image of an isolated peapod. The inset shows the electron beam used for diffraction. (b) An experimental diffraction pattern recorded from the peapod shown in (a). The arrows indicated diffraction by C60 molecules. (From[21], reproduced with permission)

A focused probe can be formed by weakening the CL lens and placing the crossover at the front focal plane of the CM lens. This results in a focused probe on the specimen, which is placed at the focal plane of the objective prefield lens. When using a small condenser aperture with a small convergence angle, the probe size becomes diffraction limited in a FEG TEM. The diffraction patterns recorded in this case consists of small disks (see Figure 10.13 for an example). This nanodiffraction technique was pioneered by Cowley [4].

10.2.3 Convergent-Beam Electron Diffraction (CBED)

CBED is recorded using a focused electron probe at the specimen. Compared to the diffraction techniques that we have discussed so far, CBED differs in terms of the beam convergence angle (θ_c) and the electron probe size. The convergence angle is several times larger than what is used in NBD, but it is still significantly smaller

than the convergence angle used in an aberration corrected STEM. The convergence angle is largely determined by the size of the condenser aperture (CA). The CA is considered to be conjugate to the diffraction pattern in CBED. Using an additional mini-lens placed above or in the objective prefield, it is also possible to vary the convergence angle by changing the strength of the mini-lens for CBED. In addition, in CBED performed using a thermionic electron source, the incident plane-wave components of the illumination are considered to be incoherently related.

The relatively large convergence angle used for CBED gives rise to transmitted and diffracted disks (see Figure 10.5 for an example); the size of the disk determines the range of excitation errors for each reflection (more in the Section on The geometry of CBED). Thus, the convergence angle is a very important parameter in CBED. Its choice depends on the application. Along a zone axis, the ideal CBED disk size is twice the Bragg angle of the lowest order ZOLZ reflection, in order to fill the diffraction space as nearly as possible with scattered rays. In an off-zone axis orientation, a large CBED disk can be used to extend the number of HOLZ lines recorded in the transmitted disk. As the desired convergence angle changes from one crystal to another or one application to another, a TEM designed for CBED provides a range of excitations of the CM lens so it can be used to vary the convergence angle as shown in Figure 10.3. The size of the CBED disk for a fixed CM lens excitation is determined by the condenser aperture size and the focal lengths of the probe-forming lenses. Experimentally, by having several condenser apertures from a few microns to several tens of microns, it is possible to cover a range of convergence angles for many materials science applications.
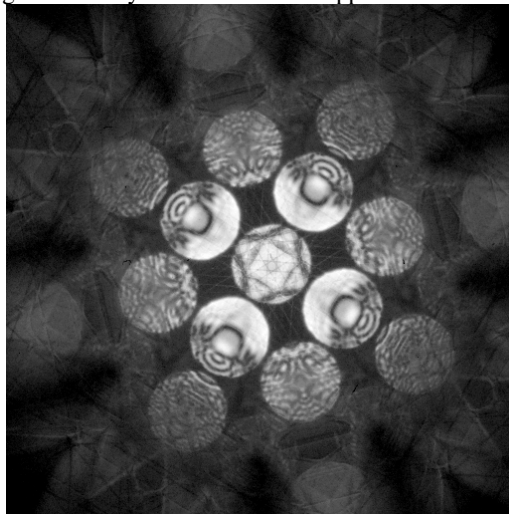
Figure 10.5 CBED pattern recorded from spinel ($MgAl_2O_4$) at 120 kV, energy filtered, using LEO 912 TEM by Syo Matsumura, Yoshitsugu Tomokiyo and Jian Min Zuo (reproduced with author's permission).

If the CA is coherently illuminated using a field emission electron source, when the coherent CBED disks are allowed to overlap, it then becomes possible to form a scanning transmission (STEM) lattice image. By observing this STEM lattice image, it thus becomes possible (in thin crystals) to stop the probe on the region at which a CBED pattern is required. It is quite possible by this method to obtain CBED patterns from different regions within a single unit cell, and that these show different site symmetries, or alternatively, by averaging over one or several unit cells, to obtain their average symmetry. In order to obtain sufficient intensity from a probe of sub-nanometer dimensions, an instrument fitted with a field-emission gun is needed for this type of work. For the analysis of perfect crystals, the most important benefit of a field-emission gun is the improved plane-wave coherence at the specimen level. This also makes it sensitive to the contributions from defects in a real crystal. However, because of the small focused probe, the pattern has reduced contributions from thickness variations, and bending under the probe.

For very thin crystals, the resulting patterns may be interpreted as electron holograms. Coherent CBED patterns formed with a very large illumination aperture have a special name, called ronchigrams. The interpretation of ronchigrams is discussed in Chapter ? on STEM, since these provide the simplest and most accurate method of aligning the instrument, and of measuring the optical constants of the probe-forming lens.
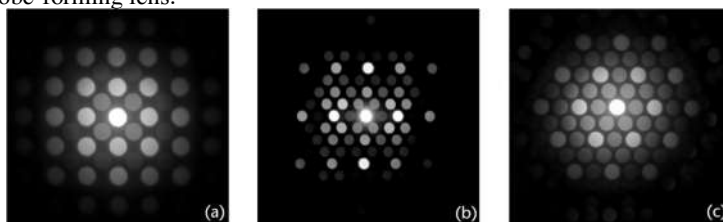

Figure 10.6 Experimental CBED patterns recorded from thin crystals of spinel (MgAl$_2$O$_4$) along zone axes of a) [100], b) [110] and c) [111]. (from [22], reproduced with permission)

CBED patterns from very thin crystals also show very little feature within each diffracted disk (see Figure 10.6 for examples). This leads to the possibility of using the average disk intensity to measure the structure factor magnitude based on the kinematic (single-scattering) theory. The angular width of the rocking curve is inversely proportional to sample thickness, so that we might expect the intensity to be constant within each disk for a sufficiently thin crystal. Such a kinematic convergent-beam (KCBED) (or "blank disk") method has been investigated ([22]), and found to have the following advantages:

(1) It allows use of the smallest electron beam diameter for solving true nano-crystal structures.

(2) Since the beam energy is spread out throughout the disks, the (000) disk intensity may be measured without saturating the detector, so that "absolute" intensity

measurements can be made, comparing the intensity of the zero-order beam with the Bragg intensities.

(3) One has a test, which is independent of the (unknown) crystal structure, for the presence of unwanted multiple scattering, if the structure is known to be non-centrosymmetric. In that case, these CBED patterns will only be centrosymmetric (in accordance with Friedel's law) if the scattering is kinematic. (Friedel's law is violated in the presence of multiple scattering).

Experimentally, one needs to obtain good quality CBED patterns from all the major zone axes of the crystal, which may be difficult for a very small nanocrystal, depending on the degree of symmetry and radiation damage limitations. Full details of the method, as used to solve the structure of a spinel crystal with about 0.03 nm resolution, are given in McKeown and Spence ([22]). Here a three-dimensional map of the crystal potential was obtained, including the positions of the oxygen atoms. To solve the phase problem, the remarkable "charge-flipping" algorithm was used (For details, see [22]. The charge-flipping algorithm is described in section 10.5.4.2.4).
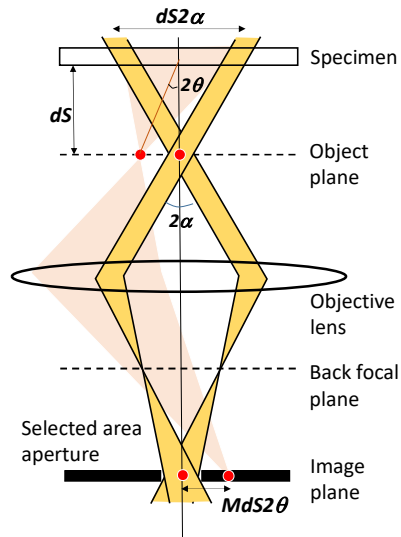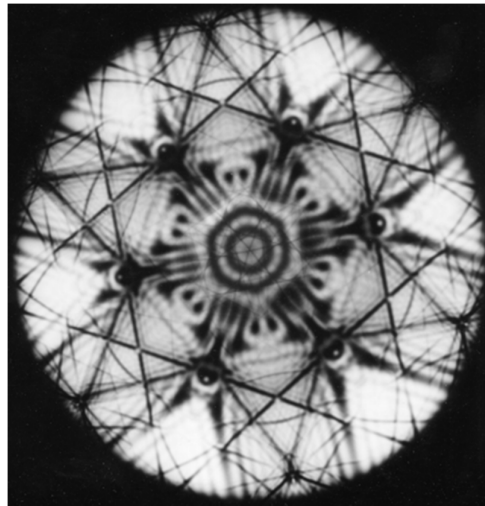
10.2.4 Large angle methods

Figure 10.7 Schematic illustration of Tanaka's LACBED method. Here α and θ denote the half convergence and Bragg angles, respectively, and M is the objective lens magnification.

Various instrumental techniques have been developed to obtain an angular view of a diffracted order which is greater than the Bragg angle. The earlier methods for

doing this have been reviewed by [23]. Such an angular expansion is required for space-group determination of crystals with a large unit cell, in which overlap of low orders may occur at such a small illumination angle θ_c that little or no rocking-curve structure can be seen within the orders. It has also been discovered that many narrow high-order reflections may be observed simultaneously using large-angle techniques.

Closely related to the large-angle methods are ronchigrams and shadow images described in the Chapter on STEM, however they differ according to the angular range over which the illumination is coherent. In this section we deal only with "incoherent" conditions, and the application of techniques used to prevent the overlap of orders.

Figure 10.8 Large angle CBED pattern recorded from Si [111] at 120 kV. (Provided by John Steeds, Bristol University)

The "Tanaka" or LACBED method (see [24]) allows parallel detection of the entire wide-angle pattern and requires no instrumental modifications. The pattern is again, however, obtained from a rather large area of sample. A description of the method is given in [25]. Figure 10.7 shows the principle of the method, while Figure 10.8 shows a pattern from (111) silicon taken at 120 kV by this method. In Figure 10.7, the CBED probe has been focused on the object plane of the objective lens, while the sample is moved up by a distance *dS*, forming an image of the electron source in the plane of the selected area aperture. A source image is formed in every diffracted order, as shown. The aperture can then be used to isolate one source image and so prevent other diffracted beams from contributing to the image. Because the source images are small at the crossover, the illumination cone can be opened up to a semiangle which is larger than the Bragg angle. The price to be paid

for this is the large area of sample illuminated by the out-of-focus probe at the sample. In addition, different regions of the sample contribute to different parts of the diffraction pattern. Patterns may be obtained with the probe focused either above or below the sample—best results seem to be obtained with it below the sample (for TEM instruments).

An important finding is that the use of the smallest selected area aperture together with the largest permissible defocus minimizes the contribution of inelastic scattering to the pattern. This effect has been studied in detail in [26]. A similar technique is used to image other diffracted orders. Here the order of interest is brought onto the optic axis using the dark-field tilt controls.

If the geometric probe size and the effects of spherical aberration are both small, the diameter D of the region from which the pattern is obtained is given approximately by

$$D = 2\alpha \, dS \tag{10.1}$$

where 2α is the beam convergence angle. The smallest dS (see Figure 10.7) which allows separation of the diffraction orders should be used to minimize D. A small geometric source image (consistent with sufficient intensity on the viewing screen) also facilitates the separation of orders—this is controlled by the demagnification settings of the condenser lenses. Applications of the above LACBED method can be found in [27]. A variation of this method has also been demonstrated which makes it possible to record simultaneously on a single micrograph most of the CBED pattern, together with several diffracted orders at the Bragg condition [28].
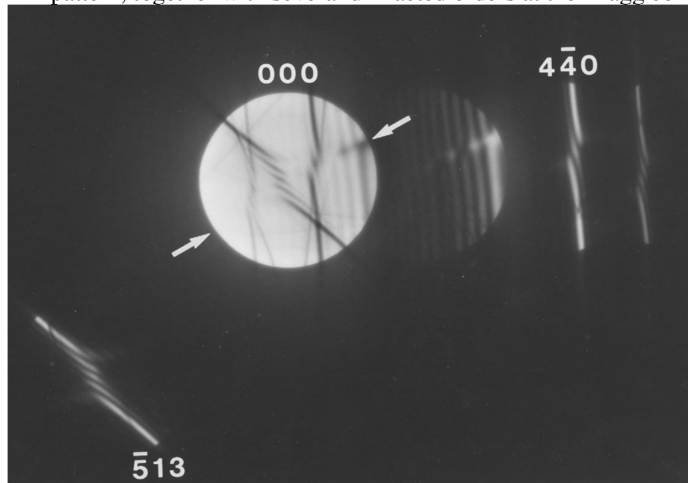
Figure 10.9 Experimental CBED pattern from silicon containing a dislocation as marked by arrows. The number of splits can be used to identify the dislocation Burgers' vector. (from [29], reproduced with permission)

For defects, the LACBED or CBED technique can characterize individual dislocations, stacking faults and interfaces (see [30-32], also Figure 10.9). For applications to surfaces and interfaces, and structure without three-dimensional periodicity, parallel-beam illumination with a very small beam convergence is required.

The LACBED techniques that we have described so far are designed to avoid the overlap of diffraction disks by recording the intensities of a single reflection. Many applications requires the intensities of multiple reflections, which can be obtained using the large-angle rocking-beam electron diffraction (LARBED) technique described by Koch [33] (also see Figure 10.10). The principle of LARBED is similar to the double rocking beam technique developed earlier [34, 35]. It works by rocking the incident beam over a certain angular range, while ensuring that the same selected area of the sample contributes to the diffraction pattern and the same diffracted beam stay on the detector. For every incident-beam direction in this angular scan the intensity of the transmitted beam or a diffracted beam is displayed on a video monitor. The differences are: 1) LARBED uses a partial descan to produce a small diffraction circle from the precession of the incident beam and 2) the diffraction rings are recorded on a CCD camera instead of a point detector as in LACBED.
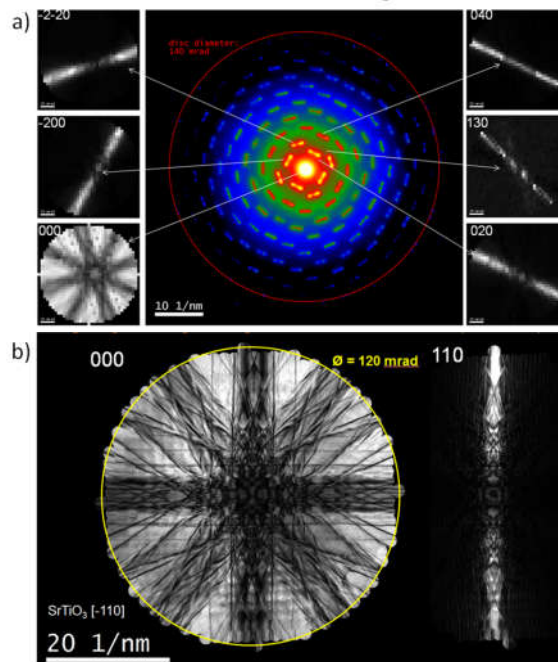
*Figure 10.10 LARBED patterns collected with a parallel beam (a) and conver-
gent beam (b). In a), for each tilt angle a separate diffraction pattern was recorded,
the integrated background-subtracted intensity for each reflection is extracted for
the corresponding beam tilt. In b), for each beam tilt a CBED pattern is recorded.
(Provided by Christoph Koch, Humboldt University of Berlin)*

10.2.5 Scanning electron nanodiffraction and scanning CBED

Using the deflection coils, scanning electron nanodiffraction (SEND) or scan-
ning CBED patterns can be recorded from an area of the sample for every probe
positions, to provide spatially resolved structural information. This can be done ei-
ther in a TEM or STEM. Diffraction patterns are recorded using a 2D digital detec-
tor, for example, a CCD camera. Compared to PACBED (section 10.2.7), which
records one diffraction pattern over many probe positions, SEND or SCBED col-
lects the full 4-D data, in the form of two spatial coordinates, the (x, y) in the real
space and the (k_x, k_y) in the reciprocal space. The only difference between SEND
and SCBED is the beam convergence angle (which is larger for SCBED). For this
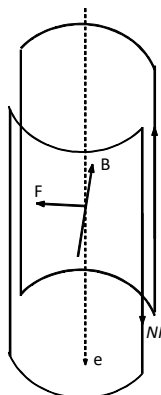reason, we will focus simply on SEND in the following discussion.

*Figure 10.11 Saddle yoke magnetic coils for electron beam deflection. A
horizontal magnetic field is produced by a pair of coils of N turns with current I
flowing in opposite directions. Electrons traveling vertically experience a force F
as shown.*

When a pair of magnetic coils (Figure 10.11) are arranged perpendicular to each
other, they apply uniform forces on the beam electrons along the horizontal (x and
y) directions. Four pairs can be used to shift or tilt the beam along any direction in
the x-y plane. Two pairs make a set of deflection coils covering the x and y direc-
tions. Double deflection coils are placed below the CL lens and above the CM lens.
They are used to provide beam shift, bright-field beam tilt and dark-field beam tilt.
When driven by an external scan generator, they are used to scan the probe in a
raster over the specimen and to form STEM images by coupling the scan together

with a detector. In electron diffraction mode, they can be configured in a number of ways for beam rocking, conical scan, as used in precession [36], and scanning electron nanodiffraction [37].

Two deflectors working in opposite senses are used to shift or tilt the beam; the individual deflector excitations are different for these two operations. Beam shift is used for SEND, and beam tilt is used in double rocking LACBED or precession electron diffraction. Figure 10.12 compares the beam shift with beam tilt using the double deflection coils in a TEM with a condenser-objective lens. For simplicity, the CM and the objective prefield lenses are shown as a single lens above the specimen. Consider a ray along the optical axis. To shift this ray at the specimen, it must be first deflected away from, and then toward, the optical axis by the first and second deflectors successively. Finally, the beam must intersect the optic axis at the front focal plane of the lens above the specimen, which then brings it to the specimen running parallel to the optical axis. To shift the beam, we actually tilt the beam. For other rays in the beam, because of the small convergence angle, the same tilt is achieved so they all converge to the same point on the specimen. The amount of beam shift is proportional to the tilt angle. To tilt the beam, it is first deflected away from the axis, and then back towards the optical axis in such a way that all rays in the beam converge to the same point on the front focal plane as undeflected rays, but now shifted laterally.
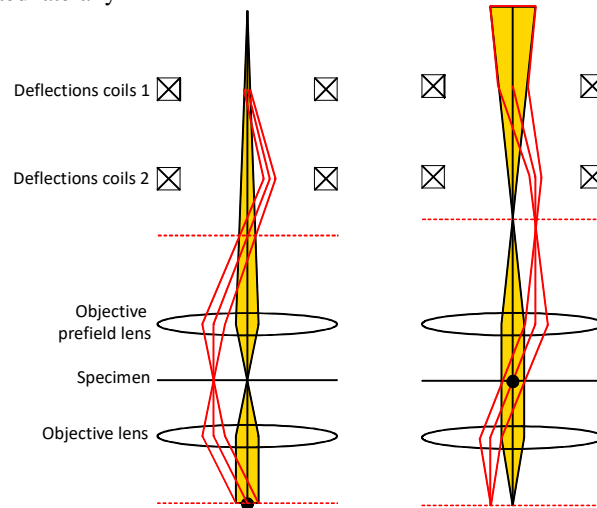

Figure 10.12 Beam deflection coils used for beam shift (left) and beam tilt (right). The dark disk marks the pivot point and dash lines mark the front and back focal planes of the prefield and objective lenses respectively.

Scanning electron diffraction can be carried out by first selecting an area of interest, dividing this area into a number of pixels, placing the electron probe at each

of these pixels and recording the diffraction patterns at each pixel [37]. Data acquisition is automated using either dedicated hardware to synchronize the scan and diffraction pattern (NanoMegas SPRL, Brussels, Belgium) or by using computer control of the TEM and the electron camera. An implementation of SEND using the second approach is reported by [38], which involves the automation of TEM deflection coils and diffraction pattern acquisition using a custom script written in the DigitalMicrograph® (DM, Gatan Inc, Pleasanton, CA) script language. The electron microscope is controlled using the script by communicating with the host processor built into the TEM. This technique does not require additional hardware other than the computer and the electron detector that are already installed on the TEM. The main drawback is that the speed of acquisition is limited by the camera readout speed or the speed of beam deflection inside the TEM, whichever is slower.
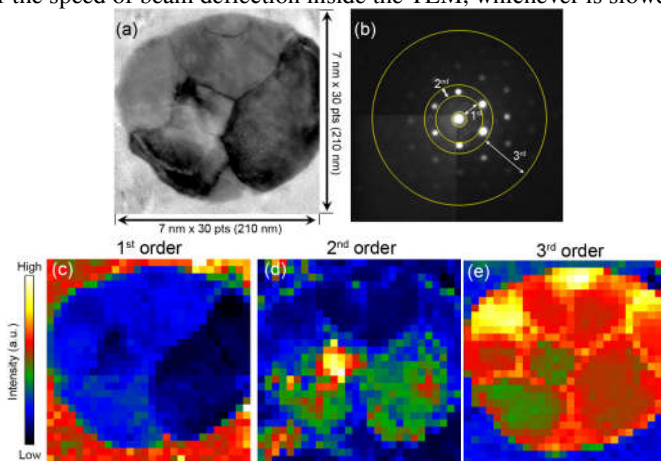

Figure 10.13 SEND of a small Au disk. (a) A BF image of nanostructured Au disk and (b) a selected diffraction pattern acquired from SEND. The diffraction intensity is integrated for the areas of 1, 2, and 3 represented in (b). The corresponding intensity maps are shown in (c), (d) and (e), respectively. (From [38], reproduced with permission)

In the method reported in [38], the electron beam scanning is performed in the TEM mode and carried out using the deflection coils to shift the beam under computer control. Two types of computer access to the TEM are used for the scanning process; the first retrieves the values of the illumination deflection coils and stores the values as real number x and y, and the second shifts the electron beam by the amount x and y. The x and y values, however, only refer to the setting of the deflection coils, which need to be calibrated into distances in nanometers. For this purpose, two scanning vectors are established along the vertical and horizontal directions. The calibration is carried out under a standard magnification in TEM mode. The reference value of (x_1, y_1) is first obtained from the initial beam position. The electron beam is then horizontally shifted to position '2', and (x_2, y_2) are obtained.

Using the calibrated magnification, the distance (*d*) between '1' and '2' can be set to a fixed value. Then, the horizontal and vertical scanning vectors are calculated. Once calibrated, the electron beam can be shifted to a specific position by a combination of the two scanning vectors.

Once the 4D dataset is collected using SEND, bright- and dark-field STEM images can be obtained simultaneously from SEND in the simplest form of analysis by integrating the diffraction intensities of the direct beam and diffracted beams respectively. In this way, SEND works like STEM. A major distinction is that with the diffraction patterns recorded and stored, other information can be extracted offline to form images, beyond the simple integrated intensities. For example, diffraction patterns can be indexed and analyzed for orientation and phase mapping (section 10.5.1.4). This analysis can be done at nm resolution, which is unique to transmission electron diffraction. This last option is simply not available using the fixed, STEM, detectors. The tradeoff here, of course, is that one will be dealing with a far more complex, and larger, data set.

Figure 10.13 shows an example of SEND applied to a nanostructured Au disk. The SEND patterns were acquired over the area of 210x210 nm^2 in 30x30 pixels, corresponding to a step size of 7 nm. Figure 10.13(b) shows one of 900 diffraction patterns acquired from SEND. The diffracted beams appear as small disks corresponding to 4.2 mrad of full convergence angle. The electron probe was formed in a JEOL TEM with the LaB$_6$ gun at the low dose condition [38]. To demonstrate the imaging capability of SEND, the diffraction intensity between two circles as marked in Figure 10.13(b) was integrated from the diffraction patterns. The intensity sum for every single diffraction pattern was then mapped in the raster image, as shown in Figure 10.13(c). For the mapping, three regions of the diffraction pattern were selected as marked in Figure 10.13 (c, d and e): (1) an annular area between the direct beam and the first ring (marked as 1), (2) the second ring (marked as 2), and (3) the remaining area of the third ring, akin to the use of an annular dark field (ADF) detector in STEM. For the first region (Figure 10.13 (c)), the amorphous region (C film) has high intensity while the Au nanodisk shows low intensity. This is expected since the amorphous scattering is strong where there are no Bragg spots from the Au nanodisk. Figure 10.13 (d) shows the variation in the integrated intensity over the grains of Au nanoparticles. This reflects the orientation change across the grains.

There are also major benefits in reducing radiation damage by using low-dose SEND to study radiation sensitive materials, including organic molecules. The work described in [39] showed that electron images recorded using illumination spots of 100 to 200 nm from thin paraffin crystals and purple membrane improve the image contrast by a factor of 3 to 5 compared to electron images taken with a large illumination spot of 3 μm. The improvement in image contrast was attributed to the reduced beam damage induced by specimen movement. In SEND, the beam damage

is limited to only area of the specimen illuminated by the electron beam and thus each diffraction pattern is recorded under nearly identical specimen condition. The new "direct electron" detectors take advantage of this effect also, by summing many very brief exposures for which the effects of beam-induced motion are corrected during data merging.
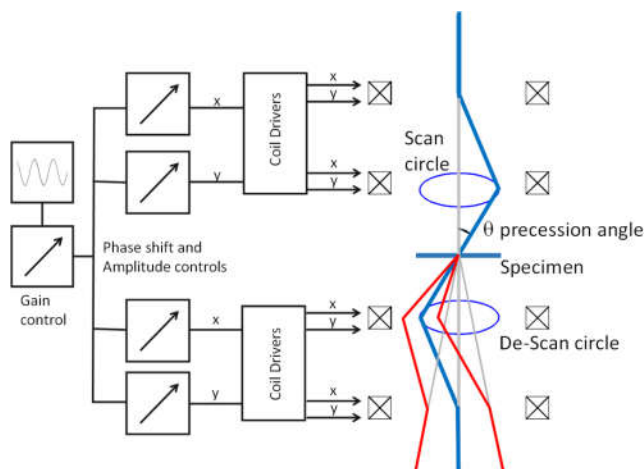
10.2.6 Precession electron diffraction

Figure 10.14 schematic illustration of precession electron diffraction setup and controls using the deflector coils above and below the specimen.

Precession electron diffraction (PED) is a technique pioneered by Vincent and Midgley [36]. The principle of the method is illustrated in Figure 10.14, in which for simplicity we have omitted the CM and condenser-objective lenses above and below the specimen. In PED, the incident electron beam is made to rotate around the microscope optical axis, maintaining a constant angle - the 'precession angle', by using the beam deflectors [40]. To compensate for motion of the diffracted beams as the incident beam rotates, the outgoing beams are deflected back using the deflectors below the specimen. The technique is similar to the double rocking technique we discussed for the recording of LACBED patterns [35], in which case the beam is made to scan over a rectangular area instead of precession around a circle. By recording electron diffraction patterns with the incident electron beam in precession, PED is able to provide the electron diffraction intensity integrated in angle across the Bragg condition for many reflections, provided that the recording time is much longer than the time it takes for one precession. Compared to CBED, which records the diffraction intensity for every incident beam directions, PED records one intensity integrated over the precession angle in a way similar to the rotational method in X-ray diffraction. It may be shown that this angular integration reduces the effects of multiple scattering, as first discussed by Blackman [41] and tested

experimentally by Horstmann and Meyer[42]. Figure 10.15 shows an example. The sample is coesite, which is a high pressure polymorph of silica with a monoclinic symmetry, space group C2/c. The diffraction patterns, one without and one with precession, were taken on two sides of a twinned crystal. The patterns are only distinguishable using precession. Especially, the kinematically forbidden 001 reflection (00h with h odd) is not visible in the precessed pattern (arrowed in Figure 10.15c). The intensity of these reflections is quite strong in the conventional pattern; their absence in the precession pattern indicates a more kinematic-like behavior for the diffraction intensity[43]. This can be understood if we imagine that there is one extinction distance (in 2-beam theory) associated with every point (every excitation error) within a CBED disk. By integrating over many such points, the precession signal averages over many extinction distances, and so smooths out the oscillations with thickness due to the Pendellosuing effect [44]. Because of this unique feature, PED has found many applications in electron crystallography for solving crystal structures.

PED is implemented by driving the x and y deflection coils before and after the specimen synchronously using the oscillating sine wave obtained from a signal generator, which is the phase shifted and amplitude adjusted for the x and y scan drivers. The same waveforms are used to drive the coils below the specimen. This is schematically illustrated in Figure 10.14. The result after careful adjustments is that, at the lower part of the beam deflector coils, the incident beam scans sequentially around a circle, which is then brought back to the specimen ideally to a fixed point so the rotating incident beam form a cone of a constant angle. Thus, a focused beam should stay focused in PED and sharp diffraction spots should stay similarly sharp.
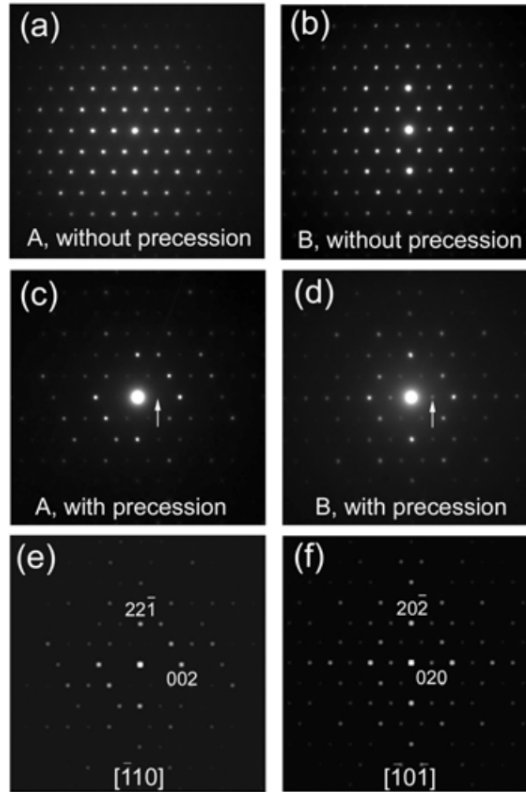
Figure 10.15 Experimental electron diffraction patterns taken from coesite (a high pressure polymorph of silica with a monoclinic symmetry, space group C2/c). Diffraction patterns marked as A and B are on each part of a twin for [1 10] and [1 01] orientations. Without precession: (a) and (b). With precession: (c) and (d). Kinematic simulated patterns: (e) and (f). (from [43], reproduced with permission)

10.2.7 Selected area diffraction in STEM

The drawback of performing SAED in a conventional TEM, where the objective lens spherical aberration limits the selected area to about 100 nm or more, can be largely avoided by performing electron nanodiffraction in a STEM. There are several ways to perform selected area electron diffraction in a STEM. Sharp diffraction spots can be obtained by using the objective prefield lens to form a small parallel probe on the specimen. The diameter of the region of the specimen with near-parallel illumination depends on the diameter of the condenser aperture. Using a small aperture (10 μm or less), the illumination may be as small as a few tens of nanometers, and diffraction pattern spots are then as sharp as these obtained by a parallel beam in a TEM. For applications where having sharp diffraction spots are not so

critical, such as phase identification or orientation mapping, a focused probe can be used with correspondingly higher spatial resolution.

The recording of SAED patterns can be made in conjunction with STEM imaging using an annular dark-field detector with a low camera length setting and a large inner cutoff angle. Because STEM imaging is performed in diffraction mode, no additional optical adjustment is needed between imaging and diffraction. Once the image is obtained, nanodiffraction patterns can be recorded in several ways:

1) By positioning the electron probe at specific specimen positions, selected based on the STEM image.
2) By applying a small, fast scan of the beam during the recording of the pattern (0.1 seconds exposure time or longer). Then, the area giving rise to the diffraction pattern can be increased significant beyond the diameter of the electron probe[4].
3) By recording scanning electron nanodiffraction patterns, which will be the subject of the next section.
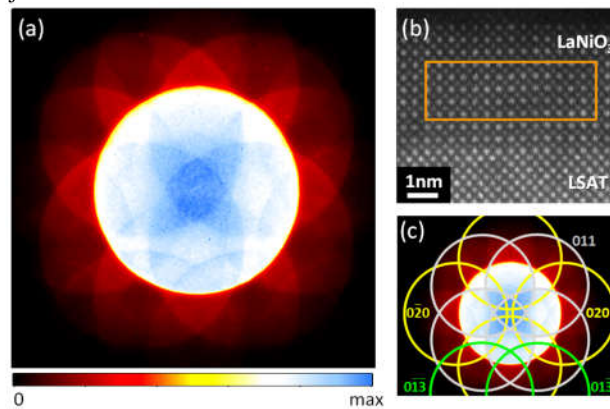

Figure 10.16 Position averaged CBED (PACBED). (a) Experimental PACBED pattern recroded by scanning the electron probe across the boxed area in (b). (b) HAADF-STEM image of a 5 nm thick LaNiO₃ film on (LaSr)AlTiO₃. (c) Same pattern as in (a), with pseudocubic Miller indices. (produced from [45] with Authors' permission)

Unlike SAED performed in TEM, the beam convergence angle is separately controlled from the selected area for electron diffraction in STEM. Because of this, some unique applications can be made. One is to acquire diffraction patterns over a small rectangular area defined by the STEM scan coils, which has special applications in atomic resolution STEM. The condenser aperture is coherently illuminated, so that large overlapping CBED disks interfere. The interference pattern changes sensitively as the electron probe moves from one atomic column to another, contributing to the image contrast observed in bright-field STEM[46]. Interpretation of

coherent CBED (or "coherent nanodiffraction") patterns, however, is complicated because we need to know the exact probe position as well as the phase of electron waves, including the phase from lens aberrations and electron multiple scattering. In this sense, the interpretation of these patterns is exactly as complicated as the interpretation of HREM images. These patterns do, however, reveal the local point symmetry of the crystal as reckoned about the center of the beam, and this effect has been used to locate the STEM probe on particular atoms, for collection of EELS spectra[47]. This method has been used to determine the atomic structure, and to classify, the anti—phase domains which occur in alloys of CuAu [48], and is reviewed by Cowley and Spence[49].

By averaging over a region of specimen, the so-called position averaged CBED (PACBED) removes all the interference between overlapping CBED disks ([45, 50]). As the example in Figure 10.16 shows, the patterns show a remarkable resemblance to CBED patterns recorded with an incoherent probe. In an aberration corrected STEM, the electron probe can be smaller than 1Å. The smallest specimen region that can be scanned in order to fully remove the coherence effect is a unit cell. The actual volume probed in a PACBED experiment depends on electron probe propagation. Since the electrons are no longer confined to a single atomic column as in a channeling situation, the actual volume is larger than the region scanned by the electron probe. Nonetheless, PACBED has the highest spatial resolution among all diffraction techniques for probing structure on the scale of the unit cell.

A major application of PACBED is the determination of crystal thickness for quantitative analysis of STEM image contrast. This technique when combined with quantitative techniques described in later chapters could be used to study local symmetry, polarization and crystal stoichiometry.

10.3   Electron probes and energy filtering

10.3.1   Probe formation

A variety of small electron probes are employed in electron nanodiffraction using coherent and "incoherent" illumination. Under "incoherent" conditions (i.e., the electron lateral coherence length is much smaller than the diameter of the condenser aperture) the total probe diameter d_o of a focused probe is given approximately at Gaussian focus by adding in quadrature the various contributions to d_o. Thus,

$$d_o^2 \; = \; d_s^2 + d_d^2 + d_{sa}^2 + d_c^2 + d_f^2 \qquad\qquad (10.2)$$

where d_s is the geometrical source image diameter, d_d is the diffraction broadening equal to $0.6\lambda/\theta_c$ with θ_c for the convergence angle, d_{sa} is the contribution from lens aberrations (in a TEM without a probe corrector, it is equal to $0.5C_s\theta_c^3$ in the plane of least confusion, not the Gaussian image plane), and d_c is the contribution from